

INFLUENCE OF SINTERING CONDITIONS ON THE MICROSTRUCTURAL AND MECHANICAL PROPERTIES OF POROUS Ti c.p. FOR BIOMEDICAL APPLICATIONS

Y. Torres ¹, J. Pavón ², I. Nieto ¹, J. A. Rodríguez ¹

¹ Department of Mechanical and Materials Engineering, University of Seville, Avda. Camino de los Descubrimientos, s/n, 41092 Seville, Spain
E-mail: ytorres@us.es

² BIOMAT Group, Bioengineering Program, University of Antioquia, Calle 67, No. 53-108, Medellín, Colombia
E-mail: jjpavon@udea.edu.co

ABSTRACT

Among all biomaterials used for bone replacement, it is recognized that both commercially pure titanium (Ti c.p.) and Ti₆Al₄V alloy are the materials that show the best *in vivo* performance due to their excellent balance between mechanical, physical-chemical and biofunctional properties. However, one of the most important disadvantages of them is their higher stiffness with respect to the bone which produces the *stress shielding* phenomenon, promoting the bone resorption around the implant with an associated risk of failure. In this work is investigated the influence of the main powder metallurgy processing parameters, compaction pressure and sintering temperature, in the porosity, stiffness and yield strength of porous commercially pure titanium (Ti c.p.) samples manufactured for reducing the stress shielding phenomenon. The results have shown that lower values of both compaction pressure and sintering temperature implies lower values of samples stiffness, as logical consequence of the higher porosity. The spherical levels of pores as well as the free mean pathway between them were increased for higher values of both compaction pressure and sintering temperature. The better stiffness results, by comparison with cortical bone, were obtained for 38.5 MPa and a sintering temperature of 1000°C. These conditions also corresponded to the better balance with respect to desired yield strength and the expectable higher fatigue resistance due to more spherical pores.

KEY WORDS: Biomaterials, Porous Titanium, Powder Metallurgy, Stress Shielding.

1. INTRODUCTION

Bone properties degradation associated to both traumas and diseases, and its replacement, is currently one of the most important public health problem. This bone damage is evident by the density reduction since the 30 years old, which implies a strength reduction up to 40% that could be increased by both the cyclic load degradation and the surface wear of joints. Of all biomaterials used for bone replacement, it is recognized that both commercially pure titanium (Ti c.p.) and Ti₆Al₄V alloy are the materials that show the best *in vivo* behaviour due to their excellent balance between mechanical, physical-chemical and biofunctional properties. However, they have three disadvantages which, in many cases, compromises the implants and prosthesis liability: 1) the stiffness of titanium is higher than the bone one which produces the *stress shielding* phenomenon, promoting the bone resorption around the implant; 2) despite its high osteointegration capability, titanium is surrounded by a fibrous tissue because of its bioinert behaviour which is related with many loosening events and 3) it is required more studies about its liability from damage prevention criteria, because this is the only admissible criteria for biomaterials design. Regarding the stress shielding problem, there are some works and developments of both biocomposites and

porous titanium implants that still not reach the suitable equilibrium between mechanical and biofunctional properties [1-4]. Several previous works have shown that is possible to match the stiffness of cortical bone by using different techniques to fabricate porous titanium samples [5-15]. However, there is a lack of studies about the real effect of this porosity on other important mechanical properties, i.e. mechanical strength and fatigue life, and also about the relationships between both the porosity and microstructure with the mechanical properties.

In this work is investigated the influence of main sintering conditions, compaction pressure and temperature, on both microstructural and mechanical properties of porous Ti c.p. samples. The powder metallurgy process used to manufacture the samples consisted of a conventional process of compaction followed by sintering of Grade 4 Ti c.p. samples. This work was developed in the framework of a project in which the aim is to evaluate the improvement of the equilibrium between biofunctional and mechanical properties of porous titanium implants designed to improve osteointegration, to reduce stress shielding and to prevent the damage.

2. EXPERIMENTAL PROCEDURE

2.1 Samples processing

The powder was previously fabricated by a hydrogenation/dehydrogenation process. The particle size distribution, according to the supplier SE-JONG Materials Co. Ltd., Corea, showed a mean size of 23.3 μm with a chemical composition equivalent to Grade 4 Ti c.p. ASTM F67-00. In order to obtain porosities between 30% and 50%, to ensure the desired stiffness [4,16-17], the compaction pressures used were 38.5, 89.7, 147.4 and 211.5 MPa (from the compressibility curve of the titanium powder), and the sintered temperatures were 1000, 1100, 1200 and 1300°C for 2 h. The powder mass used to obtain the cylindrical samples (diameter of the 12 mm) was of 5.14 g. The compaction step was carried out by using an Instron 5505 universal machine to apply the pressure needed for the desired porosity, followed by a MALICET ET BLIN U-30 universal machine in order to remove the samples from the matrix. The compaction loading rate was 600 kgf/s, the dwelling time was 2 min and the unloading time was 15 s for decreasing load up to 15 kgf. The sintering process was performed in a CARBOLYTE STF 15/75/450 ceramic furnace with a horizontal tube using high vacuum (5×10^{-4} mbar).

2.2 Density, porosity and microstructural characterization

Density and porosity (total and interconnected) measurement was carried out by using Arquimedes method with distilled water impregnation due to its experimental simplicity and reasonable reliability (ASTM C373-88). The porosity was also assessed by image analysis using an optical microscope NIKON EPIPHOT coupled with a camera JENOPTIK PROGRES C3, and a properly analysis software (IMAGE-PRO PLUS 6.2). This analysis was performed only in the middle part of the cylinders because it presents theoretically the most homogeneous pores distribution. Before the image analysis, the sectioned part was properly prepared by a sequence of conventional steps (resin mounting, grinding and polishing) followed by a mechano-chemical polishing with magnesium oxide and hydrogen peroxide. The porosity parameters estimated by this method were the convexity (convex perimeter/pore perimeter), form factor ($F_f = 4\pi A/PE^2$, where A is the pore area and PE is the experimental perimeter of the pore), mean free path between the pores, the porosity itself, maximum and mean area of pores, grade of contiguity of the pores, equivalent diameter, elongation factor and pores density. Conventional optical microscopy (OM) and scanning electron microscopy (SEM) were also used for the basic observation of the microstructural features of the samples.

2.3 Mechanical testing

For mechanical compression testing, smaller cylinders were machined from the central part (more homogeneous) of the original sintered cylinders, following the recommendations of the Standard ASTM E9-89a (height/diameter = 0.8). The tests were carried out with a universal electromechanical Instron machine 5505 by applying a strain rate of 0.005 (mm/mm·min). All tests were considered finished for a strain of 50% and, afterwards, it was estimated both Young modulus, E , and yield strength, σ_y . The Young modulus estimation from the compression stress-strain curves was corrected with the testing machine stiffness (87.9 kN/mm). The dynamic Young modulus measurement using the ultrasound technique was performed with a KRAUTKRAMER USM 35 equipment, which was used to estimate both longitudinal and transverse propagation velocity of acoustic waves. For each case it was used the properly probe PANAMETRICS and a suitable ultrasonic couplant fluid. Once the acoustic wave velocities and densities are measured, the dynamic Young modulus calculation is made by using a proper mathematical expression. Finally, the Young modulus of porous samples were also estimated by a calculation made from both porosity and pores form factor measurements, using the model proposed by Nielsen [18].

3. RESULTS AND DISCUSSION

3.1 Samples processing

Fig. 1 shows an example of the sample aspect after the sintering process for compaction pressure and sintering temperature of 38.5 MPa and 1300°C, respectively.



Fig. 1. Porous Ti c.p. PM material (38,5 MPa and 1300 °C) and machined in three pieces.

None of the sintered samples showed any phenomena of oxidation and contamination of titanium, which is a clear indicator of the role played by the vacuum during sintering. Also, as it was mentioned previously, all characterization and mechanical testing was focused in the central part of the cylinders because of its porosity uniformity.

3.2 Density, porosity and microstructural characterization

Fig. 2 shows the dependence of both total and interconnected porosity, in terms of both compaction pressure and sintering temperature.

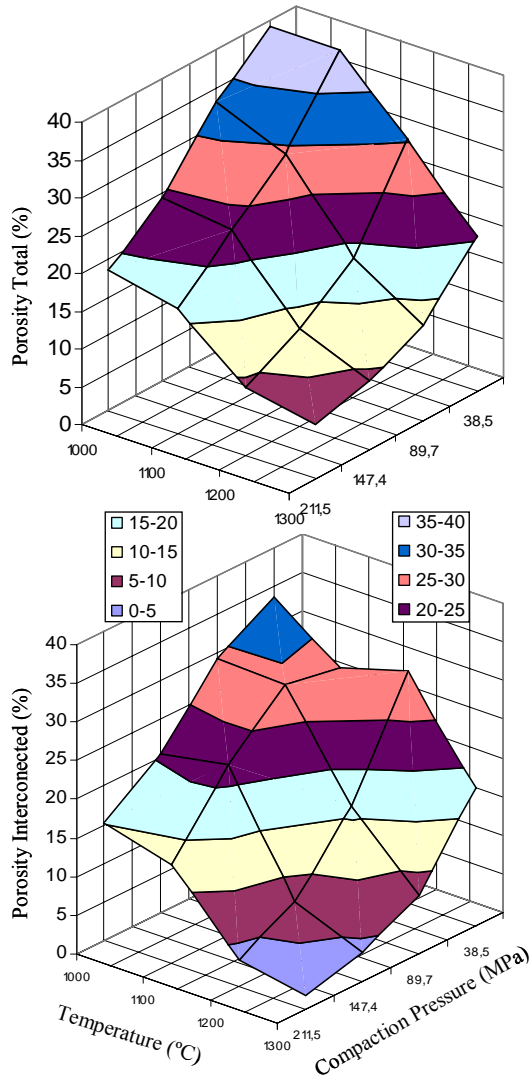


Fig. 2. Porosity behaviour as a function of both compaction pressure and sintering temperature.

As it was expected, the lower values of total porosity, and higher density, were obtained for the higher values of both compaction pressure and sintering temperature. Regarding the total porosity range guide to reach the desired stiffness, according to previous works (30% and 50%), this was obtained for compaction pressure values between 35.8 MPa and 89.7 MPa and sintering temperatures between 1000°C and 1200°C as can be clearly observed in the figure 2. From this it can be inferred that for a total porosity range of 30% to 40% and a sintering temperature range of 1000°C to 1200°C, it can be used a compaction pressure range of 38.5 MPa to 89.7 MPa, with higher porosity values for both lower compaction pressure and sintering temperature. With respect to interconnected porosity behaviour, it presents

the same trend as the total porosity. However, in this case there is not a defined desired range because it will depend on the elastic properties of the material to be used as filler compound (bioactive glass, high-density polyethylene, etc.). In fact, this kind of porosity should be most properly controlled to be only at the surface in order to promote the bone ingrowth, considering the risk of reducing both mechanical strength and fatigue resistance.

In Fig.3 it is summarised the behaviour of the pores morphology parameters in terms of both compaction pressure and sintering temperature. From these results it can be noticed, as it was expected, that the most important parameters, form factor (F_f) and free-mean path or distance between pores (λ), increased for higher values of both compaction pressure and sintering temperature. As a logical consequence, porosity was reduced (higher stiffness) especially by compaction pressure effects, as sintering temperature has stronger influence in F_f . However, the most important feature of the pore morphology behaviour is the different trend of both F_f and λ parameters for lower and higher compaction pressure: it is observed that for a fixed low compaction pressure (38.5 MPa) an increasing sintering temperature has a stronger effect in both F_f and λ , with a small porosity reduction, than for a fixed higher compaction pressure (211.5 MPa). This trend implies that, in order to improve both mechanical and fatigue resistance with a small effect in the desired porosity (stiffness), it is advisable to work with small sintering temperature increments for the lowest compaction pressure which is consistent with the stronger effect in F_f due to an increasing sintering temperature. Sintering temperature increments for highest compaction pressure produce largest pores due to coalescence of the smallest ones present at lowest temperatures.

3.3 Mechanical testing

The compression stress-strain curves of the samples for the different processing conditions are depicted in Fig.4. From this figure it is verified that an increment in sintering temperature, for a fixed compaction pressure, implies higher values of both Young modulus and yield strength. However, it is interesting to remark the different sensitivity to sintering temperature depending on the compaction pressure level: it is clear that both E and σ_y are more sintering temperature sensible for the lowest compaction pressure which is clearly consistent with the higher sintering temperature sensitivity observed previously for porosity parameters (F_f and λ). This result indicates that F_f and λ not only can affect plastic properties (yield and mechanical strength, and fatigue resistance) but also the elastic properties of the titanium porous sample. Therefore, this has to be considered in order to improve the mechanical properties of porous titanium without any important effect on the stiffness of the sample.

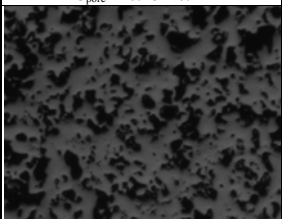
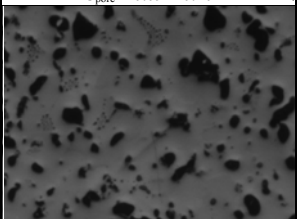
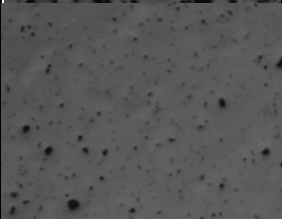
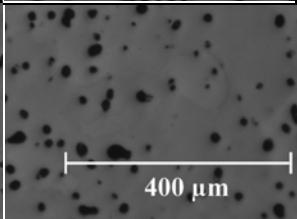
	1000 °C	1100 °C	1200 °C	1300 °C
38.5 MPa	$P(\%) = 41.3 \pm 2.5$ $F_t = 0.81 \pm 0.25$ $A_{med} = 484 \pm 1575 \mu m^2$ $\delta_p = 757 \pm 108 \text{ poros/mm}^2$ $\lambda = 38.4 \pm 30.8 \mu m$ $C_{pore} = 0.26 \pm 0.09$	$P(\%) = 44.2 \pm 3.1$ $F_t = 0.80 \pm 0.26$ $A_{med} = 698 \pm 2144 \mu m^2$ $\delta_p = 693 \pm 125 \text{ poros/mm}^2$ $\lambda = 31.7 \pm 27.0 \mu m$ $C_{pore} = 0.18 \pm 0.11$	$P(\%) = 30.5 \pm 1.6$ $F_t = 0.85 \pm 0.21$ $A_{med} = 325 \pm 630 \mu m^2$ $\delta_p = 740 \pm 28 \text{ poros/mm}^2$ $\lambda = 54.0 \pm 33.8 \mu m$ $C_{pore} = 0.09 \pm 0.10$	$P(\%) = 18.3 \pm 2.9$ $F_t = 0.91 \pm 0.16$ $A_{max} = 6042 \pm 1045 \mu m^2$ $\delta_p = 554 \pm 54 \text{ poros/mm}^2$ $\lambda = 89.1 \pm 32.9 \mu m$ $C_{pore} = 0.10 \pm 0.19$
89.7 MPa	$P(\%) = 35.6 \pm 2.4$ $F_t = 0.84 \pm 0.23$ $A_{med} = 244 \pm 535 \mu m^2$ $\delta_p = 1134 \pm 129 \text{ poros/mm}^2$ $\lambda = 38.7 \pm 22.4 \mu m$ $C_{pore} = 0.08 \pm 0.10$			$P(\%) = 10.2 \pm 1.4$ $F_t = 0.93 \pm 0.14$ $A_{med} = 200 \pm 248 \mu m^2$ $\delta_p = 497 \pm 70 \text{ poros/mm}^2$ $D = 134.9 \pm 25.7 \mu m$ $C_{pore} = 0.09 \pm 0.13$
147.4 MPa	$P(\%) = 22.3 \pm 1.1$ $F_t = 0.95 \pm 0.12$ $A_{med} = 89 \pm 118 \mu m^2$ $\delta_p = 755 \pm 73 \text{ poros/mm}^2$ $\lambda = 127.1 \pm 45.4 \mu m$ $C_{pore} = 0.02 \pm 0.07$			$P(\%) = 7.1 \pm 0.8$ $F_t = 0.96 \pm 0.10$ $A_{med} = 172 \pm 168 \mu m^2$ $\delta_p = 439 \pm 29 \text{ poros/mm}^2$ $\lambda = 158.5 \pm 56.6 \mu m$ $C_{pore} = 0.01 \pm 0.04$
211.5 MPa	$P(\%) = 17.0 \pm 1.4$ $F_t = 0.96 \pm 0.10$ $A_{med} = 60 \pm 88 \mu m^2$ $\delta_p = 705 \pm 160 \text{ poros/mm}^2$ $\lambda = 176.0 \pm 23.1 \mu m$ $C_{pore} = 0.04 \pm 0.1$	$P(\%) = 14.6 \pm 1.1$ $F_t = 0.96 \pm 0.11$ $A_{med} = 81 \pm 116 \mu m^2$ $\delta_p = 652 \pm 134 \text{ poros/mm}^2$ $D = 162.0 \pm 39.0 \mu m$ $C_{pore} = 0.05 \pm 0.13$	$P(\%) = 7.6 \pm 2.1$ $F_t = 0.97 \pm 0.10$ $A_{med} = 73 \pm 87 \mu m^2$ $\delta_p = 279 \pm 184 \text{ poros/mm}^2$ $D = 401.2 \pm 204.4 \mu m$ $C_{pore} = 0$	$P(\%) = 5.6 \pm 0.8$ $F_t = 0.97 \pm 0.08$ $A_{med} = 183 \pm 168 \mu m^2$ $\delta_p = 431 \pm 41 \text{ poros/mm}^2$ $\lambda = 161.7 \pm 44.4 \mu m$ $C_{pore} = 0.04 \pm 0.10$

Fig. 3. Effects of the temperature and compaction pressure in characteristic of the pores.

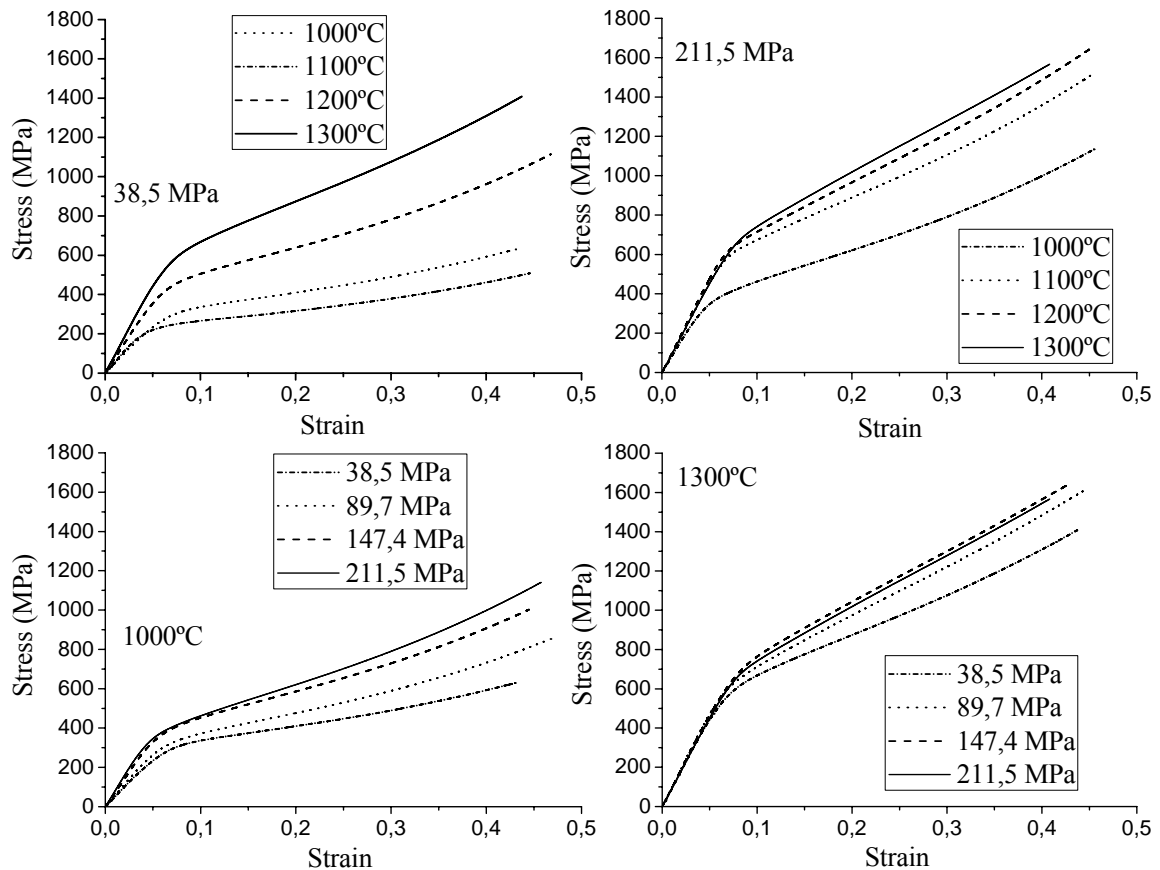


Fig. 4. Compression stress-strain curves of the samples for the different processing conditions.

Note, from the same figure, that compaction pressure increment for lowest and highest sintering temperatures show the same E and σ_y sensitivity: they are more sensible for compaction pressure increments at the

lowest sintering temperature. Regarding the searched stiffness value for cortical bone replacement ($E_{CB} \approx 20 \text{ GPa}$).

Fig. 5 shows that the better results (20 to 25 GPa) were obtained for the lowest compaction pressure (35.8 MPa) with sintering temperatures of 1000 and 1100°C, corresponding to the highest porosity (~ 40 %). In this figure are also included the trends obtained by other authors and it is noticed that their results fix reasonably well with those obtained in this work. Finally, it should be mentioned that yield strength values, corresponding to the better stiffness results, were always higher than the cortical bone one.

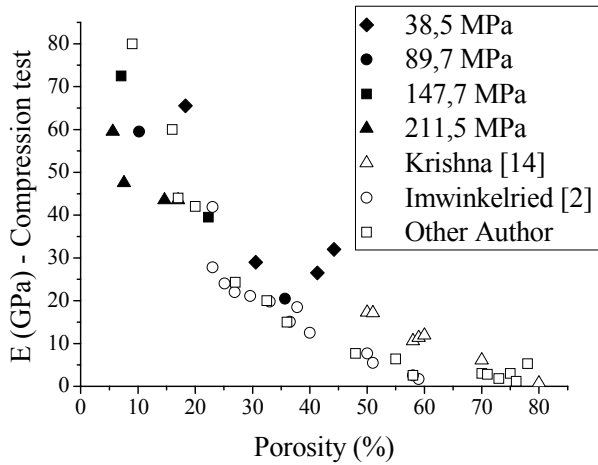


Fig. 5. Behaviour of Young modulus by compression test in terms of total porosity. Relation between the compression young modulus and porosity.

From Fig. 5 it is noticed the influence of using the stiffness correction of testing machine in Young modulus evaluation: corrected values are higher for same porosity. However, these values remain lower than those obtained with the ultrasound technique as can be observed and discussed later.

The Young modulus measurements obtained by ultrasound technique (dynamic Young modulus) showed a higher values trend than those estimated from the compression stress-strain curves (see Figs. 5 and 6). However, for the lowest Young modulus values the results are more similar. These differences could be explained due to normal uncertainties of the compression test measurement and also because of the higher well known reliability of the ultrasound technique.

The theoretical curves which are included in Fig. 6 correspond to mathematical expressions that relate Young modulus with porosity: Gibson and Ashby [19] is used for compression test estimation and Pabst-Gregorova [20] and Knudsen are for ultrasound data. Note that ultrasound technique measurements of this work are in well concordance with theoretical estimations...

In Fig. 6 is presented the dynamic Young modulus behavior in terms of compaction pressure, sintering temperature and porosity. As in the case of the

compression test measurement, the better stiffness results correspond to both lowest compaction pressure and sintering temperature (35.8 MPa and 1000°C - 1100°C) with a porosity of approximately 40 %. Note that the relation between measurements, compression test and ultrasound, and porosity are in well concordance with those reported in previous works [2,14, 20]: 20 MPa to 25 MPa for 50% of porosity. Despite the better stiffness results obtained in this work were for lowest sintering temperature, this does not imply any detriment of mechanical strength as could be expected from the literature. In fact, the authors are currently developing a new work in which they are using lower compaction pressure (13 MPa) and even loosing sintering, with such a good results as 50% porosity and 14,3 GPa for 1000°C, and 45% porosity and 21,7 GPa for 1200 °C.

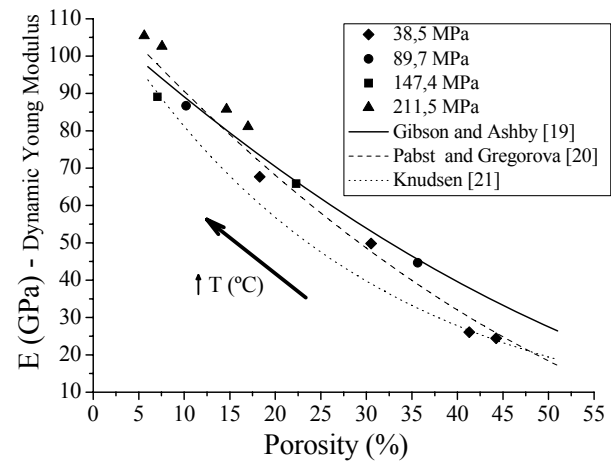


Fig. 6. Relation between the dynamic Young modulus and porosity.

Similar stiffness values for lower porosity could be explained due to some measurement uncertainties in the previous works (all compression test measurements in this work were corrected with the testing machine stiffness) and also because the ultrasound technique study was carefully and detailed carried out. In fact, the reliability and certainty of the ultrasound measurements were contrasted and validated by comparison with well known and accepted pore-elasticity model like Nielsen one [18]: Fig. 7 presents the adjust between the both Young modulus experimental measurements and the calculation by using the Nielsen model including porosity parameter experimentally determined. Nielsen model is given by the following expression:

$$E_p = E_{Ti} \frac{\left(1 - \frac{P}{100}\right)^2}{1 + \left(\frac{1}{F_f} - 1\right) \left(\frac{P}{100}\right)} \quad (1)$$

where E_{Ti} is the Young modulus of Ti porous free, P is the total porosity and F_f is form factor of the porous sample. From Fig. 7 it is evident that Young modulus measurements from ultrasound technique present the best fit with respect to calculations from Nielsen

model, for the complete range of both compaction pressure and sintering temperature. On the other hand, measurements obtained from compression test, in this work and also in some previous study, show an important deviation for highest Young modulus values.

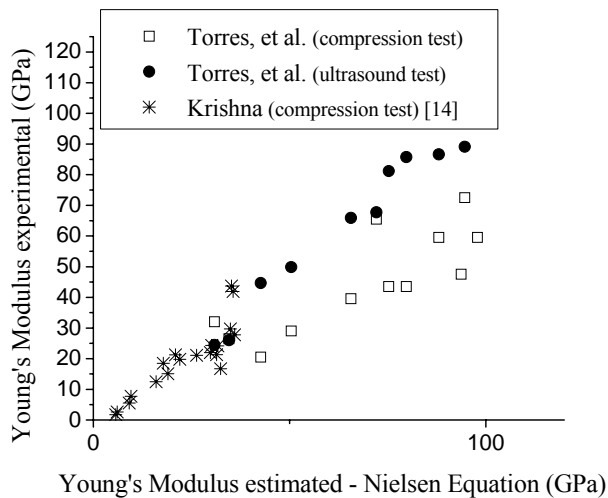


Fig. 7. Comparison of Young modulus measurement by different methods with the calculation by estimated Nielsen equation.

4. CONCLUSIONS

According to the results of the study about the influence of conventional powder metallurgy conditions in both microstructural and mechanical properties of porous Ti for bone replacement, the following salient findings can be drawn:

1. The better stiffness results of porous Grade 4 Ti cp porous samples for cortical bone replacement (20 to 25 GPa against to aprox. 20 GPa of bone) were obtained for the lowest values of both compaction pressure and sintering temperature (38.5 MPa and 1000°C -1100°C), with a porosity of approximately 40 %. These results correspond to the central part of cylindrical samples initialled fabricated, due to its highest porosity uniformity.
2. The main porosity parameters, form factor and mean free path, presented a highest sensitivity to sintering temperature increments for a lowest compaction pressure. This trend was consistent with the behavior exhibited by both Young modulus and yield strength from compression tests: highest sensitivity for sintering temperature increments at lowest compaction pressures as well as for compaction pressure increments for lowest sintering temperatures. The knowledge of this sensitivity could be determinant in order to improve both mechanical strength and fatigue life with a low influence in the porosity and, therefore, in the stiffness of the samples.
3. Ultrasound technique used for dynamic Young modulus estimation of porous Ti samples has shown to be a suitable tool for the study of this

kind of materials. This was reasonably verified by comparison of the measurements obtained by this technique with the values calculated from a theoretical model like Nielsen one, which include porosity parameters experimentally determined.

ACKNOWLEDGMENTS

The authors wish to thank to the laboratory technicians J. Pinto and the student J.M. Recio for carrying out the microstructure characterization and mechanical testing.

REFERENCES

- [1] Gerard, D. A. and Koss, D. A., International Journal of Fatigue, 13 (2): p. 345-352, 1991.
- [2] Imwinkelried, T., Journal of Biomedical Materials Research - Part A, 81 (4): p. 964-970, 2007.
- [3] Yue, S., et al., Journal of Biomedical Materials Research, 18 (9): p. 1043-1058, 1984.
- [4] Oh, I. H., et al., Scripta Materialia, 49 (12): p. 1197-1202, 2003.
- [5] Ryan, G., et al., Biomaterials, 27(13): p. 2651-2670, 2006.
- [6] Dunand, D. C., Advanced Engineering Materials, 6(6): p. 369-376, 2004..
- [7] Asaoka, K., et al., Journal of Biomedical Materials Research, 19(6): p. 699-713, 1985.
- [8] Spoerke, E. D., et al., Journal of Biomedical Materials Research - Part A, 84(2): p. 402-412, 2008.
- [9] Dewidar, M. M. and Lim, J. K., Journal of Alloys and Compounds, 454(1-2): p. 442-446, 2008.
- [10] Wenjuan, N., Chenguang, B., GuiBao, Q., Qiang, W., Materials Science and Engineering: A, 506(1-2): p. 148-151, 2009.
- [11] An, Y. B., et al., Materials Letters, 59(17): p. 2178-2182, 2005.
- [12] Orrù R., Licheri, R., Locci A.M., Cincotti, A., Cao, G., Materials Science and Engineering: R: Reports, 63(4-6): p 127-287, 2009.
- [13] Traini, T., et al., Dental Materials, 24(11): p. 1525-1533, 2008.
- [14] Krishna B.V., Bose, B., Bandyopadhyay, A., Acta Biomaterialia, 3: p. 997-1006, 2007.
- [15] Ryan, G. E., et al., Biomaterials, 29(27): p. 3625-3635 2008.
- [16] Wang, J. F., et al., Journal of Materials Processing Technology, 197(1-3): p. 428-433, 2008.
- [17] Spoerke, E. D., Murray, N. G., Li, H. L., Brinson, L. C., Dunand, D. C. and Stupp, S. I., Acta Biomaterialia, 1(5): p. 523-533, 2005.
- [18] Nielsen LF., J Am Ceram Soc., 67(2): p. 93-8,1984.
- [19] Gibson, L.J. and Ashby, M.F., Cellular Solids: Structure and Properties, second edition, Cambridge University Press, 1997.
- [20] Pabst, W. and Gregorová, E., J. Mater. Sci., 39: p. 3501, 2004.
- [21] Knudsen, F.P., J. Am. Ceram. Soc., 44: p. 376, 1959.